
Since January 2020 Elsevier has created a COVID-19 resource centre with free information in English and Mandarin on the novel coronavirus COVID-19. The COVID-19 resource centre is hosted on Elsevier Connect, the company's public news and information website.

Advances in Clinical Radiology 3 (2021) 103–124
ADVANCES IN CLINICAL RADIOLOGY

# Emerging Pulmonary Infections in Clinical Practice

**Jennifer Ann Febbo, MD*, Loren Ketai, MD**
Department of Radiology, University of New Mexico, 2211 Lomas Boulevard Northeast, Albuquerque, NM 87106, USA

**KEYWORDS**
• Emerging infections • Pulmonary infection • Computed tomography

**KEY POINTS**
- Severe acute respiratory syndrome coronavirus-2 and H1N1 influenza are both immunologically novel viruses that can cause an organizing pneumonia pattern of lung damage and have similar imaging findings.
- Other emerging and reemerging pathogens, such as human metapneumovirus and legionella typically cause bronchopneumonia and multifocal segmental or lobar pneumonia, respectively, which appear similar to other community-acquired pathogens.
- Emerging diseases can also be chronic infections, such as nontuberculous mycobacterium and chronic aspergillosis, which cause significant morbidity and mortality.

*Mighty things from small beginnings grow.*
—JOHN DRYDEN

## INTRODUCTION

The severe acute respiratory syndrome coronavirus-2 (SARS-CoV-2) consists of only 4 proteins. One of which, the spike protein, recently achieved a configuration that binds the human cell Angiotensin 2 receptor effectively [1]. That small adaptation has helped propel the emergence of SARS-CoV-2 and thereby change the world. The emergence of some other pathogens also hinges on subtle interactions between virus and host cell surfaces, for example, influenza's differential affinity for the sialic acid found on the cells of humans compared with that on cells of birds. Other pathogens reemerge due to changes in climate, changes in public health measures, or changes in demographics. Resurgence of dengue fever in the Caribbean, South America, and more recently the United States, is a well-known result of these forces [2]. Rising incidence of coccidioidomycosis, nontuberculous mycobacteria, and chronic aspergillosis may also be driven by developing changes in environment and human populations.

In this article, we discuss a few common emerging and reemerging respiratory pathogens. Some of these pathogens, SARS-CoV-2, influenza, human metapneumonvirus (HMPV), legionella, and coccidioidomycosis cause acute illness. Nevertheless, although the current pandemic has biased our concept of emerging disease toward acute infections, emerging pathogens can also cause chronic disease. Coccidioidomycosis spans both acute and chronic presentations, and nontuberculous mycobacteria and chronic aspergillosis are exclusively chronic processes. For these examples, we attempt to focus on imaging findings that can assist diagnosis or provide important guides to therapy.

## CORONAVIRUS DISEASE 2019 PNEUMONIA

We have learned an immense amount about SARS-CoV-2 (commonly referred to as Coronavirus Disease 2019

*Corresponding author, *E-mail address:* jfebbo@salud.unm.edu

https://doi.org/10.1016/j.yacr.2021.04.010
2589-8701/21/ 

or COVID-19) and learned it at a faster pace than possible for any pathogen in human history. Typical and atypical imaging findings of COVID-19 pneumonia on both chest radiographs and computed tomography (CT) have been skillfully described, including suggestions for structured reporting to accompany specific findings [3,4]. Typical radiographic findings include multifocal bilateral peripheral opacities, rounded opacities, and basilar predominance (Fig. 1). Atypical findings that suggest an alternative diagnosis include lobar consolidation, solitary lung nodule or mass, diffuse micronodules, edema pattern, and cavity formation [5].

Rigorous study of chest CT in multiple nations has given rise to several COVID-19 scoring systems, which largely converge on important findings. Many of the typical imaging findings correspond with an organizing pneumonia pattern of lung injury [6] (Fig. 2). For instance, the COVID-19 Reporting and Data System (CO-RADS) and the Radiolgocial Society of North America (RSNA) classification system similarly define typical CT features of multifocal ground glass opacities, with or without consolidation, in a subpleural distribution; the RSNA system noting that atoll sign may be present later in the acute presentation of disease (Fig. 3). Confining diagnosis to patients with typical findings results in specificities in the 90% to 95% range with sensitivities in the 65% to 70% range [7]. Broadening inclusion criteria to include intermediate CT findings increases sensitivity to 90% to 95% and suppresses specificity to 70% to 75%.

Interestingly, in one meta-analysis the false negative polymerase chain reaction (PCR) rate was lower among patients with atypical imaging findings for COVID-19 than among those patients with negative CTs, approximately 6% versus 14%. This may relate to the higher likelihood of an alternative, non-COVID-19 cause of symptoms in patients with atypical abnormalities, whereas patients with completely negative CTs could include those in very early stages of SARS-CoV-2 infection. Few studies have directly compared cohorts with COVID-19 to specific infections. One study of multiple radiologists showed a median sensitivity of 80% and specificity of 93% in differentiating COVID-19 from multiple other viral pneumonias [8]. Differentiation from H1N1 influenza may be more difficult (see later in this article).

Although most patients with COVID-19 pneumonia demonstrate characteristic imaging findings, most clinical sites rely on reverse PCR testing rather than imaging for diagnosis. False negative PCRs can occur, but the likelihood of a missed diagnosis of COVID-19 is markedly diminished if a second PCR is performed 24 hours after the first [9]. Rather than playing an important role in diagnosis, imaging of early-phase COVID-19 could become clinically relevant to prioritizing patients for treatment regimens, such as plasma therapy, which preferentially benefit patients early in the course of their disease [10]. In addition, recognition of the predominant imaging finding of organizing pneumonia pattern of lung injury has supported current use of corticosteroids in the treatment of patients with COVID-19 lung disease.

Much clinical CT imaging of seriously ill patients with COVID-19 is currently driven by suspicion of pulmonary embolic disease. Compared with other seriously ill patients, these thrombi preferentially involve segmental and smaller vessels [11,12]. At least some of these thrombi may be products of endothelial damage via viral spike protein binding to angiotensin-converting enzyme 2 (ACE-2) receptors [13]. Accordingly, some clinical guidelines have recommended pulmonary CT angiogram be considered in seriously ill

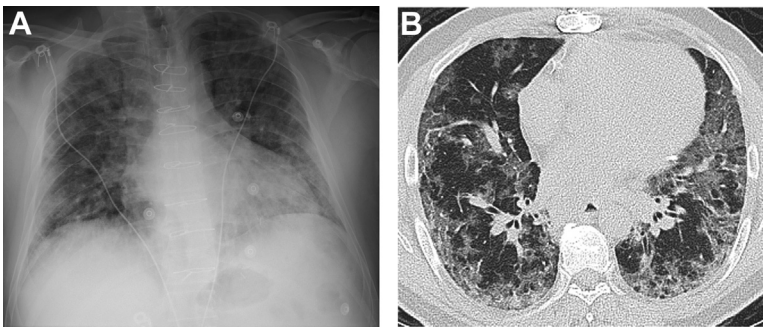


FIG. 1 Acute typical appearance of COVID-19 in a 50-year-old man. Frontal chest radiograph (**A**) shows bilateral perihilar and peripheral hazy airspace opacities without pleural effusions. Axial chest CT (**B**) demonstrates bilateral peribronchovascular and peripheral ground glass opacities.

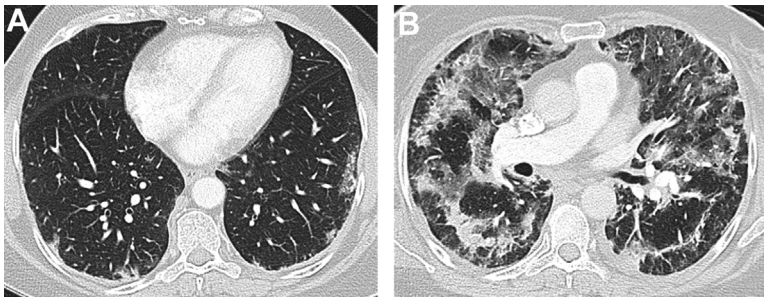


FIG. 2 Progression of COVID-19 in a 60-year-old woman. Axial chest CT on initial presentation (**A**) with very mild peripheral ground glass opacities. Axial chest CT obtained 3 weeks later (**B**) now shows extensive bilateral peribronchovascular and peripheral ground glass opacities and consolidation, with areas of subpleural sparing and perilobular pattern similar to organizing pneumonia.

patients with COVID-19 with D-dimer levels exceeding 2000 mg despite prophylactic anticoagulation. Independent of pulmonary emboli, vessel dilatation is present in most patients with COVID-19 pneumonia, likely representing a nonthrombotic manifestation of vascular pathology (Fig. 4) [14].

Although risk of thromboembolic disease is high, initial data suggest that the likelihood of bacterial coinfection is overall low in the early phases of disease [15]. Serial imaging in COVID-19 has demonstrated a peak in extent of abnormalities between 9 to 13 days. Although worsening of imaging abnormalities with onset past that expected peak could represent delayed superinfection, this has not been systemically studied. As opposed to superinfection, air block phenomena, pneumothorax, and pneumomediastinum have been shown to be common among severely ill patients with COVID-19 [16] (Fig. 5). The reason for the latter is uncertain.

Preliminary studies of convalescent disease have shown favorable imaging results for patients with mild to moderate disease, but persistent CT abnormalities in patients with severe disease requiring mechanical ventilation. A study of patients with mild to moderate disease who did not require mechanical ventilation demonstrated complete resolution of

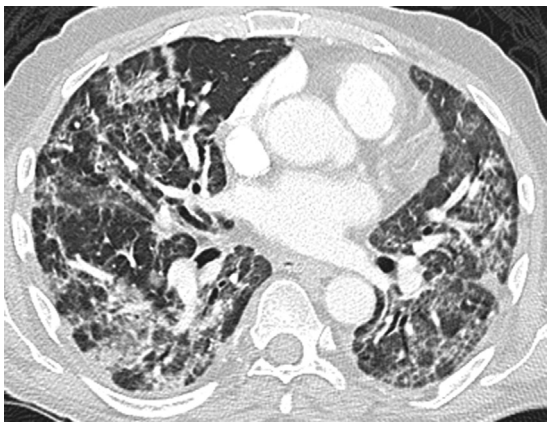

FIG. 3 Reverse halo in a 62-year-old man with COVID-19. Axial chest CT shows an area in the anterior right middle lobe of central low attenuation and peripheral high attenuation, the "reverse halo," or "Atoll," sign. Extensive bilateral ground glass and focal consolidative opacities in a peripheral and peribronchovascular pattern, as well as perilobular pattern, are also seen.

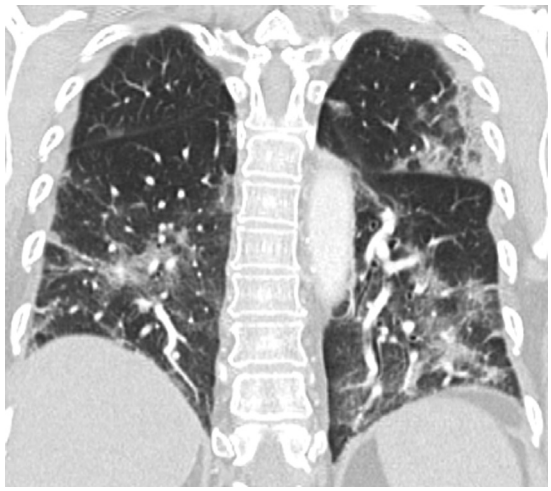

FIG. 4 Vessel dilation in a 62-year-old woman. Coronal chest CT demonstrates dilated pulmonary arteries that reach the lung periphery. Bilateral peripheral and peribronchovascular ground glass opacities are also present.

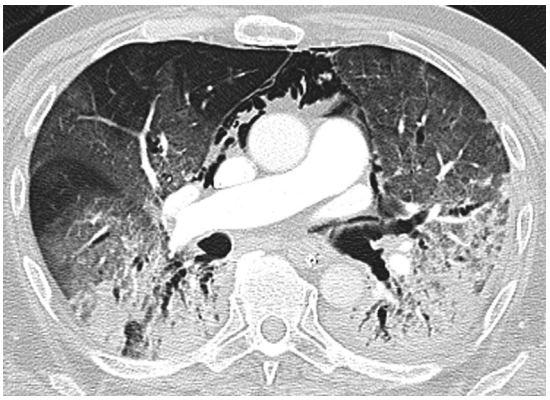

FIG. 5 Barotrauma in a 68-year-old man with COVID-19. Axial chest CT demonstrates extensive pneumomediastinum. Bilateral peribronchovascular and peripheral ground glass opacities, consolidation, and bronchiectasis are seen, compatible with the patient's COVID-19 infection.

pulmonary opacities on 48-day follow-up CT [17]. In a different study of follow-up CTs 4 months after initial presentation, only a minority of patients with mild to moderate disease (13%) demonstrated persistent mosaic attenuation, reticulation, and/or architectural distortion [18] (Figs. 6 and 7). In contrast, most (52%–66%) patients with severe disease in this study demonstrated these persistent abnormalities. Other studies have also shown persistent, fibroticlike changes predominantly in patients with severe disease. One 6-month follow-up study of CTs of patients who had been hospitalized for COVID-19 pneumonia has found that 35% of patients demonstrated fibroticlike changes (traction bronchiectasis, parenchymal bands, and/or honeycombing) [19]. These residual abnormalities were associated with prior acute respiratory distress syndrome, treatment with noninvasive mechanical ventilation, and age older than 50.

As the follow-up post-infection interval remains relatively short (months rather than years), it is not known whether these changes are permanent and reflect irreversible fibrosis. Perhaps more important, it is yet unknown whether residual imaging abnormalities correlate with clinically significant symptoms, which are common. For instance, a study of 143 patients showed that a large majority (87.4%) reported at least 1 persistent symptom 60 days after the onset of initial symptoms, the most commonly reported symptoms were persistent fatigue and dyspnea [20].

## H1N1 PNEUMONIA

The long-term fate of SARS-CoV-2 among the human population is uncertain; however, that of influenza is not. Influenza will always be with us. Influenza A, which is the usual source of epidemic influenza is subtyped on the basis of 2 surface proteins, Hemagglutinin (H) and Neuraminidase (N). A total of 9 H and 16 N exist. All of these can be found in waterfowl, whereas humans are usually only infected with H1-H3 and N1-N2. When viruses with different subtypes infect the same cell, genetic re-assortment can yield virus surface antigens novel to the human population that are capable of initiating an epidemic [21].

To add complexity, not all hemagglutinins or neuromanidases with the same numeric designation are immunologically identical. In 2009, an H1N1 variant arose that contained a unique combination of influenza genes not previously identified in animals or humans. The H1N1 (2009) virus was sufficiently different from recent prior H1N1 such that few young people had

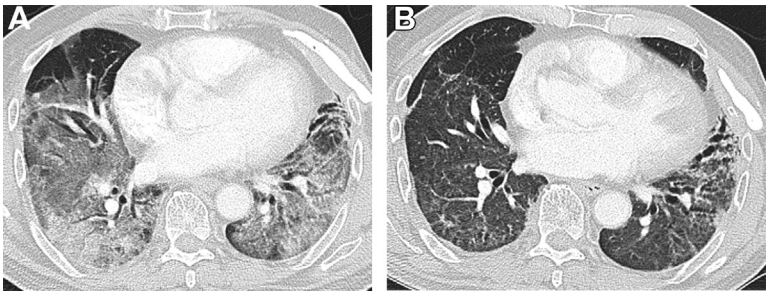


FIG. 6 Convalescent COVID-19 in a 71-year-old man. Axial chest CT from initial hospitalization (**A**) shows extensive bilateral ground glass opacities and mild bronchiectasis in the lingula. (**B**) Follow-up CT performed 4 months later demonstrates significant improvement in the ground glass opacities, but with increased bronchiectasis in the lingula and left-greater-than-right lower lobes.

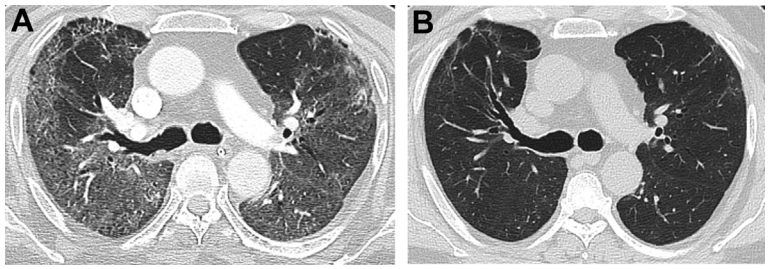


FIG. 7 Convalescent COVID-19 in a 62-year-old man. Axial chest CT images from initial hospitalization (**A**) demonstrate bilateral peribronchovascular and peripheral ground glass opacities with areas of perilobular pattern. Mild traction bronchiectasis is also seen in the anterior upper and lower lobes. Follow-up CT image performed 9 months later (**B**) shows essential resolution of the ground glass opacities, with mild residual perilobular pattern. The bronchiectasis has also improved overall.

existing antibodies, compared with one-third of people older than 60 years (likely from exposure to an older H1N1 virus earlier in their lives). During its first year of spread, H1N1 infected more than 60 million individuals in the United States [22]. Globally, 80% of H1N1(2009) virus-related deaths occurred in people younger than 65 years, as opposed to typical seasonal influenza epidemics, during which approximately 70% to 90% of deaths occur in people 65 years and older. Forms of the H1N1(2009) virus have continued to circulate worldwide, and as of 2018, the Centers for Disease Control and Prevention (CDC) estimated it that it had infected approximately 100 million people in the United States and caused approximately 75,000 deaths [22].

In addition to immunogenicity, the H1N1(2009) virus differed in respiratory cell binding characteristics. The H protein is responsible for viral cell binding that occurs at surface receptors containing sialic acid, which can have an α2-6 or and α2,3 linkage to galactose. The former pattern is found in the tracheobronchial pseudocolumnar epithelium in upper and lower airways, whereas the latter is present in terminal bronchioles, type 1 pneumocytes, and alveolar macrophages. Most human influenza viruses bind preferentially to the α2-6 receptors, but H1N1(2009) influenza binds well to both α2-6 and α2,3 sialic [21].

During the 2009 H1N1 epidemic, most patients also presented with normal chest radiographs. In those with more severe disease, radiographs demonstrate patchy opacities with a lower lobe and central predilection [23] (Fig. 8). In general, H1N1(2009) pneumonia CT findings were similar to those seen in other influenza A viruses. In general, on CTs of influenza A pneumonia, bilateral irregular areas of ground glass and consolidation are often visible, typically in a peribronchial distribution [24] (Figs. 9 and 10). Centrilobular nodules can also be present, but usually not to the extent seen with some other viruses, such as human metapneumovirus and respiratory syncytial virus [25,26]. In addition to peribronchial opacities, however, some patients with H1N1(2009) demonstrated extensive ground glass opacities in subpleural distribution, suggesting organizing pneumonia [27] (Fig. 11).

The H1N1 influenza circulating worldwide today can present with extensive subpleural ground glass opacities similar to those described in the initial outbreak, and accordingly CT images can appear very similar to COVID-19 pneumonia. Comparison of the currently circulating H1N1 influenza to COVID-19 pneumonia did not show significant differences between these pathogens in extent of peribronchovascular or subpleural ground glass or consolidation [28]. Patients with H1N1 were less likely to demonstrate a crazy paving pattern or to demonstrate vascular enlargement. Nevertheless, the imaging appearance of H1N1 influenza and SARS-CoV-2 are sufficiently similar that distinguishing these pathogens will depend on laboratory testing rather than CT.

Both H1N1(2009) pneumonia and SARS-CoV-2 pneumonia tend to produce more severe infections among obese patients. This most likely represents obesity's impairment of both innate and adaptive immune systems to combat viral infections in general, rather than a defect in combating these specific pathogens. A predilection toward pulmonary emboli was also reported in patients with H1N1(2009) pneumonia during the epidemic, but no predilection toward peripheral emboli was noted [23]. Neither have additional signs of vascular pathology, such as the local vessel enlargement seen in SARS-Cov-2, been described in H1N1 [28]. This may reflect the absence of specific

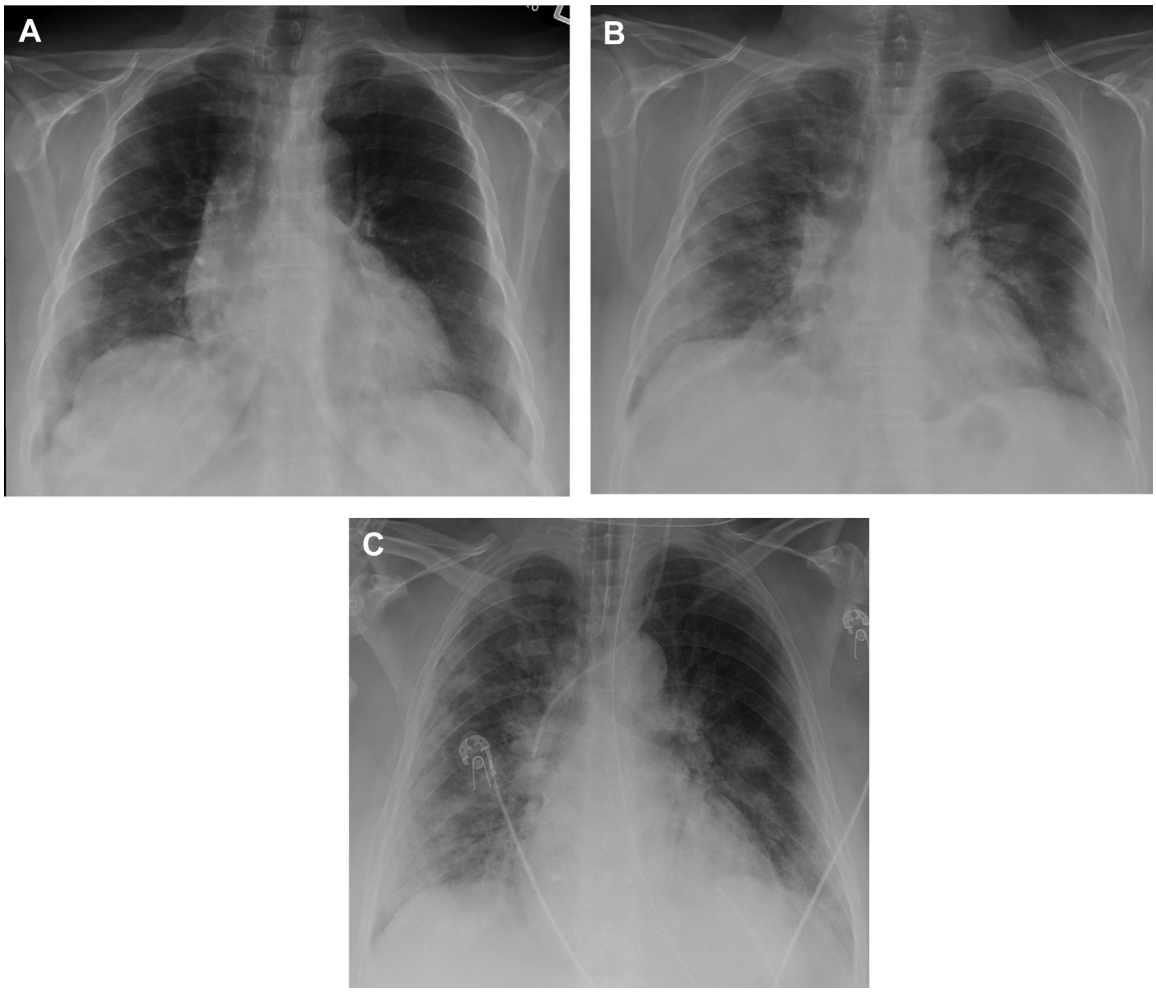


FIG. 8 . Progression of H1N1 influenza in a 58-year-old woman. Initial frontal chest radiograph (**A**) demonstrates mild bilateral, right-greater-than-left peripheral hazy airspace opacities. Chest radiographs obtained 2 (**B**) and 3 (**C**) days later demonstrate increasing bilateral hazy airspace opacities with progressive perihilar involvement.

tropism of H1N1 for lung endothelium given its lack of ACE-2 receptor binding.

## HUMAN METAPNEUMOVIRUS

Human metapneumovirus is an illustration that interspecies transmission of viral respiratory illnesses is not a phenomenon new to the twentieth and twenty-first centuries. Although the virus was only first described in 2001, phylogenetic analysis indicates it originated from avian metapneumovirus 200 to 400 years ago [29,30]. The virus has since evolved to adapt to its human host, to the degree that the human form can no longer affect birds. Its adaptation to the human host has been excellent, such that nearly all of us have been infected by age 5 [31].

Immunity is dependent on both antibodies and T cells, but the virus has various mechanisms to blunt the immune system response, including the upregulation of program cell death receptors on T cells. Accordingly, immunity is not lifelong. Most recurrent infections are mild; however, elderly adults (>65 years old) with comorbidities such as asthma and chronic obstructive pulmonary disease (COPD) are particularly

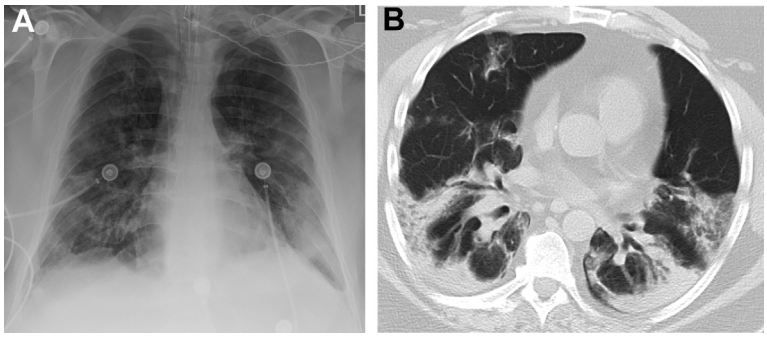


FIG. 9 Forty-four-year-old man with H1N1 influenza. Frontal chest radiograph (**A**) shows bilateral perihilar and peripheral hazy opacities. On axial chest CT (**B**), there are peripheral and peribronchovascular ground glass opacities and consolidation.

susceptible to the virus. Pneumonia may occur in up to 40% of HMPV infections in this population [32]. Mortality of outbreaks of HMPV in skilled nursing homes has exceeded 10%.

Even though the minority of HMPV infections outside the elderly population present with pneumonia, the virus is sufficiently widespread to be a significant cause of adult pneumonia in multiple age groups. This is particularly true during seasonal spikes, which usually occur 1 to 2 months after the peak of influenza. Among adults 18 to 49 years of age hospitalized for pneumonia, infections with HMPV are more common than *Streptococcus pneumoniae*, mycoplasma, *Staphylococcus aureus*, and legionella [33]. Coinfection with other viral pathogens (such as respiratory syncytial virus) is common, but it is unclear whether the presence of an additional pathogen alters the clinical course of the disease [32]. Coinfection with bacteria also occurs, pneumococcal infection being documented in a quarter of adults requiring intensive care unit admission [34] (Fig. 12).

Radiologic findings in HMPV are in keeping with its viral pedigree. Like other members of the paramyxovirus family, respiratory syncytial virus and parainfluenza, it shows a predilection for causing airway centric disease, manifest by bronchial wall thickening, bronchiolitis, and bronchopneumonia. Compared with the other paramyxoviruses, HMPV appears to be associated with more common presence of a bronchopneumonia pattern [25,35] (Fig. 13). This airway centric ground glass and consolidation differs from the alveolar filling seen with adenovirus, which often occurs without accompanying imaging findings of an airway centric process (Fig. 14).

Standard treatment for HMPV pneumonia remains supportive. Trials of vaccines and treatment with intravenous antibodies have thus far been largely confined to animal studies.

## LEGIONELLA

Unlike many of the emerging diseases causing acute respiratory symptoms, Legionnaires' disease (LD), the generally accepted term for legionellae infection, is not an epidemic disease. Instead, it manifests as sporadic disease and in environmentally triggered

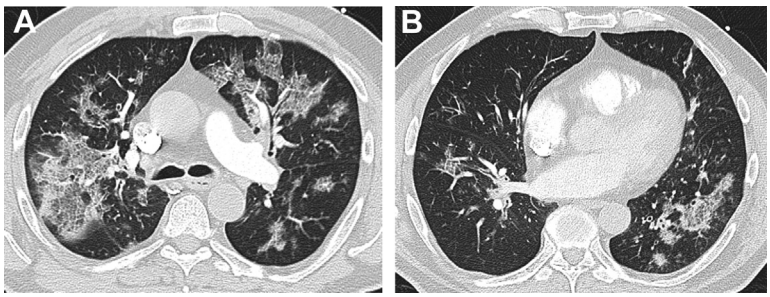


FIG. 10 Sixty-six-year-old man with H1N3 influenza. Axial chest CT images (**A, B**) show bilateral peribronchovascular ground glass opacities in a pattern similar to organizing pneumonia. Bronchial wall thickening is also apparent in the lower lobes (**B**).

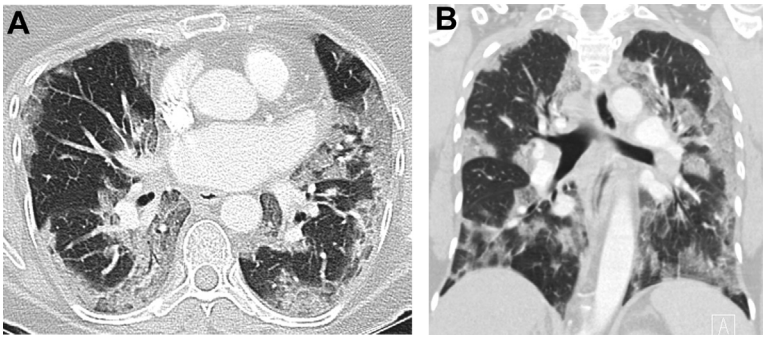


FIG. 11 Fifty-two-year-old woman with H1N1 influenza. Axial (**A**) and coronal (**B**) CT images show peripheral and peribronchovascular ground glass opacities in a pattern similar to organizing pneumonia.

outbreaks. Epidemiologically, LD is a water-borne disease. Legionellae are aerobic, gram-negative gammaproteobacteria that live in freshwater environments and infect and replicate within human alveolar macrophages [36]. Cases of LD have increased in the United States by approximately ninefold since 2000 [37]. In a 2014 US study, LD was second only to nontuberculous mycobacteria (NTMB; see chronic infections later in this article) as a cause of death from water-borne diseases [38]. The incidence of sporadic LD in the central and northeastern United States has increased from 0.45 per 100,000 in 2002 to approximately 1 to 3 per 100,000 in 2014 [39,40]. Compared with other community-acquired pneumonias, sporadic LD is more likely to lead to hospitalization and in some series is the third most common pathogen among patients hospitalized with pneumonia [41]. Indicative of this severity, LD pneumonia has a relatively high mortality rate of 10%.

Although perennially a pathogen to be considered in daily clinical practice, LD periodically becomes newsworthy during environmentally triggered outbreaks. Recent outbreaks of the disease include an outbreak of 90 cases in Genesee County, Michigan, in 2014, 58 cases in Bresso, Italy, in 2018, and 13 cases within an academic hospital in Wisconsin in 2018 [42–44]. During 2015, New York City experienced a large outbreak of LD: 138 cases with 16 deaths associated with a contaminated cooling tower [45].

Although LD is described by some as an "atypical pneumonia," its imaging characteristics are in general indistinguishable from other community-acquired bacterial pneumonias [41,46]. Consolidation and ground glass opacities are the most common findings, and can be intermixed, bilateral, and affect multiple lobes. Radiologic appearance usually continues to worsen during the first week despite the administration of appropriate antibiotics [47] (Fig. 15). Centrilobular nodules

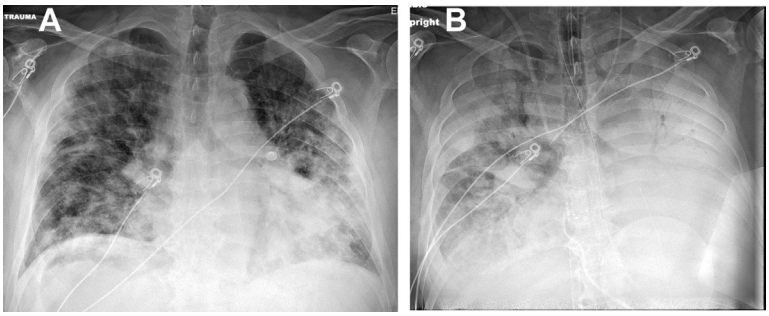


FIG. 12 Superinfection of HMPV with legionella. Frontal chest radiograph in a 71-year-old man (**A**) on presentation shows bilateral ground glass opacities. Chest radiograph on day 2 (**B**) shows rapid progression with complete opacification of the left lung and extensive ground glass opacities and consolidation in the right lung.

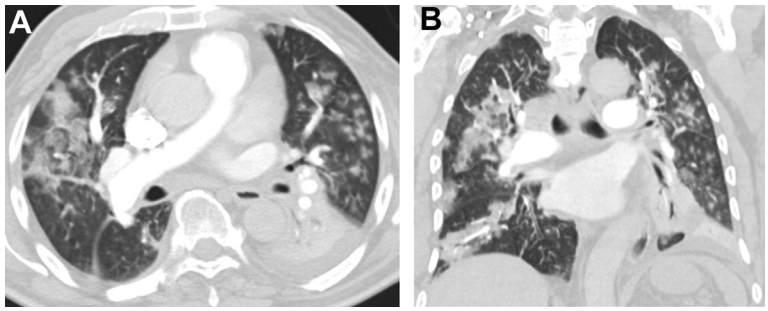


FIG. 13 Sixty-three-year-old man with human metapneumovirus (HPMV). Axial (**A**) and coronal (**B**) chest CTs show bilateral peribronchovascular ground glass opacities, centrilobular nodules, and left lower lobe consolidation.

are uncommon in patients with LD and could be a distinguishing characteristic between LD and mycoplasma and viral pneumonias; however, a direct comparison has not been made [48] (Fig. 16). Parapneumonic pleural effusions are seen in approximately half of patients, but empyema is rare and likely carries a poor prognosis [49].

Less common findings include crazy paving, interlobular septal thickening, and the reverse halo sign [50,51]. As suggested by the finding of the reverse halo sign, LD can be an etiology of organizing pneumonia [52] (Fig. 17). Although immunocompetent and immunocompromised patients in general have similar imaging findings in LD, the latter patients more commonly develop cavitary legionella pneumonia [53].

The laboratory diagnosis of LD is imperfect. The CDC recommends testing for LD with both urinary antigen testing and culture of lower respiratory secretions (eg, sputum, pleural fluid, bronchial aspirates, bronchiolar lavage). The most widely available urinary antigen tests detect *Legionella pneumophila* (Lp1) species; however, other *Legionella* species (such as *Legionella micdadei*) also cause pneumonia and can result in a false negative test. Other urine antigen tests that do detect non-Lp1 species have lower sensitivities [36]. Although culture is the gold standard, sensitivity ranges from less than 10% to 80% due to differences in sample types and laboratory experience, and some patients with LD may be unable to produce sufficient sputum for testing [36]. Nucleic acid amplification tests such as PCR for LD have been more recently developed; however, are not yet widely available for clinical use. In light of the preceding, a negative urine antigen does not definitively exclude LD in the setting of a hospitalized patient with imaging signs of progressive bacterial pneumonia. This is particularly true in patients who have suspected LD due to clinical signs and symptoms such as altered mental status, hyponatremia, and rhabdomyolysis [50].

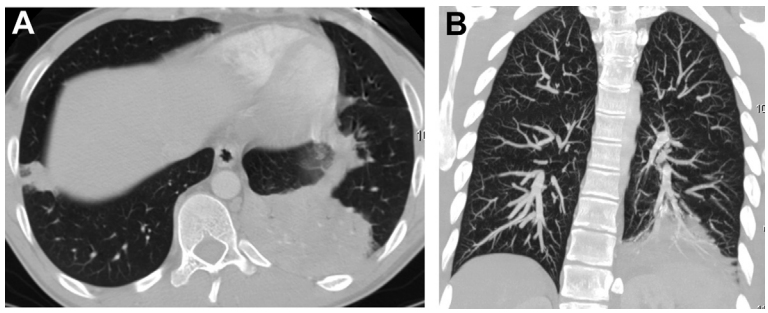


FIG. 14 Adenovirus pneumonia in a 40-year-old man. Axial (**A**) and coronal maximum intensity projection (MIP) (**B**) chest CT images show right lower lobe consolidation. The MIP images underscore the absence of centrilobular nodules.

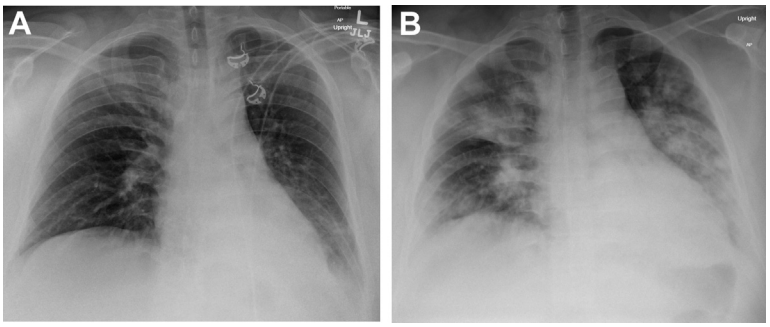


FIG. 15 Progression of legionella in a 33-year-old man. Initial chest radiograph (**A**) demonstrates a left retrocardiac consolidation. Chest radiograph obtained 3 days later (**B**) shows marked progression with new multifocal bilateral consolidation.

## COCCIDIOIDOMYCOSIS

*Coccidioides immitis* and *Coccidioides posadaii* are 2 fungal organisms that each can cause coccidioidomycosis, infections that can present as acute pneumonia, like the organisms discussed previously (Table 1). Alternatively, the infection can have more chronic manifestations. As a whole, disease caused by *Coccidioides* has increased in incidence by more than a factor of 5 between 2000 and 2018. In 2018, 15,611 cases were reported to the CDC; however, this is felt to be underrepresenting the true number of cases in the United States. Coccidioides is endemic to California, Arizona, New Mexico, and Mexico; however, its territory is growing and has been found in relatively newer regions such as northwest New Mexico near the Four Corners, northeast Utah, and Eastern Washington State [54,55]. As the disease has increased in incidence, it has been observed that non-white are at particular risk of severe infection. Of any ethnic group, Native Americans and Alaskan Natives had the highest hospitalization rate from coccidioides infection [56]. Increased rates of disseminated infection are seen in African American, Filipino, and Pacific Island ethnicities [57].

Pulmonary coccidioidomycosis can manifest as an acute pneumonia that can be difficult to distinguish from other etiologies of community-acquired pneumonia. The most common radiographic finding of coccidioidomycosis is unilateral or bilateral consolidation most commonly involving the perihilar regions and lower lobes. Hazy opacities also may be present. Nodules can be seen, but often are better visualized on CT. Lymphadenopathy is seen in only approximately 20% of chest radiographs; however, can be seen in up to 40% of patients on CT [57] (Fig. 18). CTs also demonstrate lobar or segmental consolidation, with or without ground glass opacities, satellite nodules, and cavitary nodules. Acute coccidioidomycosis can manifest solely as a solitary or multiple 0.5 to 2.5-cm well-circumscribed nodules. Pleural effusions are seen in 15% to 20% of patients and are usually

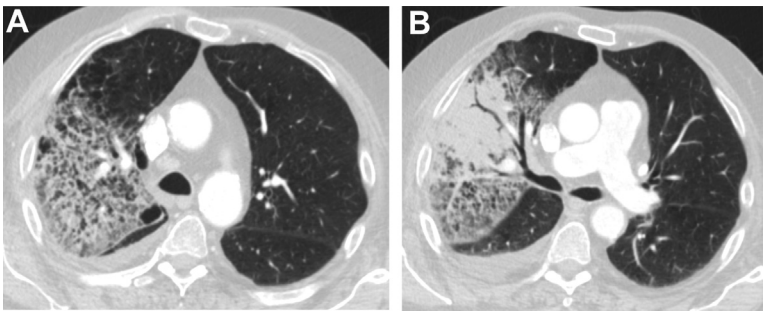


FIG. 16 Legionella in a 68-year-old man with underlying emphysema. Axial chest CTs (**A, B**) demonstrate right upper lobe ground glass opacities, consolidation, and a small right pleural effusion, with an absence of centrilobular nodules. There is a background of centrilobular emphysema.

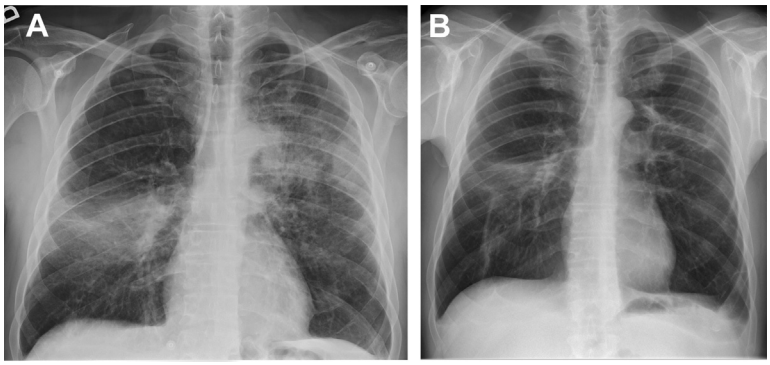


FIG. 17 Legionella in a 53-year-old man. Initial chest radiograph (**A**) demonstrates left upper lung and right mid lung consolidation. Follow-up radiograph 3 months after treatment (**B**) shows persistent opacities, with bandlike consolidation in the left upper lung and more organized, contracted consolidation in the right mid lung. These opacities may represent organizing pneumonia.

unilateral and small. Rarely cavitating nodules can rupture into the pleural cavity, resulting in empyema and potentially bronchopleural fistula (Fig. 19).

Acute coccidioidomycosis is self-limited in most patients and does not require antifungal therapy. Imaging findings that are usually sufficient to prompt antifungal therapy include bilateral consolidation, pleural effusion, and evidence of disseminated disease [57]. Concurrent risk factors, such as untreated human immunodeficiency virus/AIDS, organ transplantation, biologic response modifier therapies, diabetes mellitus, severe cardiopulmonary dysfunction, and (possibly) African or Filipino ancestry also warrant initiation of treatment [58].

Disseminated acute coccidioidomycosis usually occurs through hematogenous spread and results in miliary nodules throughout both lungs (Fig. 20). In addition, coccidioidomycosis can involve essentially any part of the body, but the most common extrathoracic sites of disease include osteomyelitis and synovitis, soft tissue infections, peritonitis, and meningitis.

Chronic coccidioidomycosis is defined as symptomatic or radiologic disease that persists for more than 6 weeks. The most common finding is a residual

**TABLE 1**
**Acute Emerging Thoracic Infections**

| Organism | Typical Imaging Finding | Additional Imaging Findings | Epidemiology |
|---|---|---|---|
| SARS-CoV-2 | Peripheral and/or bronchocentric ground glass and consolidation | Barotrauma, pulmonary embolic disease | Pandemic |
| H1N1 influenza virus | Peripheral and/or bronchocentric ground glass and consolidation | Less likely than COVID-19 to manifest vessel enlargement or crazy paving | Recurring epidemic |
| HMPV | Bronchopneumonia and bronchiolitis pattern | OP pattern uncommon | Seasonal, peak after influenza peak |
| Legionella *pneumophilia* | Multifocal consolidation | Can progress radiologically during first week of effective treatment | Sporadic, environmental outbreaks |
| *Coccidioides* (acute) | Lobar and segmental consolidation | Adenopathy <20% on CXR; more common on CT | Endemic, environmental outbreaks |

*Abbreviations:* COVID-19, Coronavirus Disease 2019; CT, computed tomography; CXR, chest radiograph; HMPV, human metapneumovirus; OP, organizing pneumonia; SARS-CoV2, severe acute respiratory syndrome coronavirus-2.

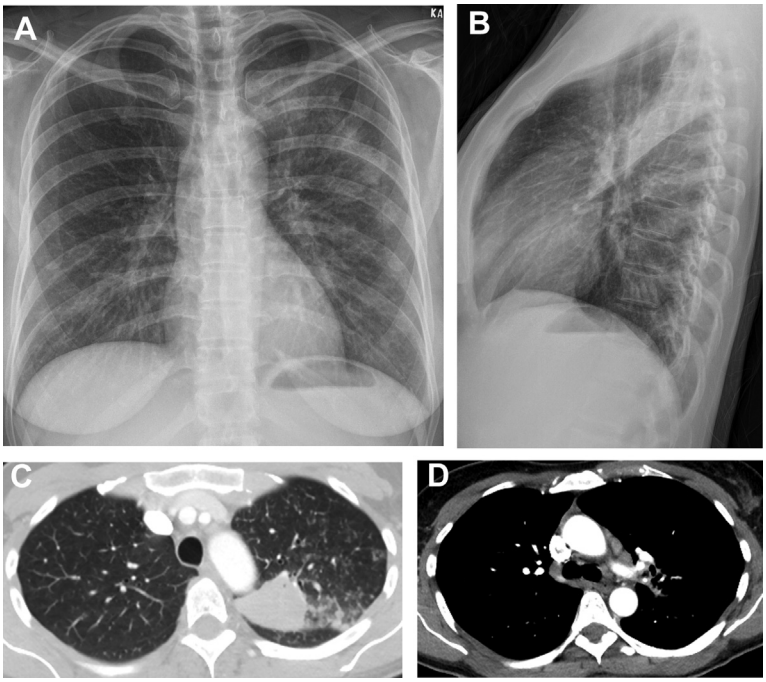


FIG. 18 Fifty-two-year-old woman with recent travel to California, presenting with fever and cough, found to have coccidioidomycosis. Posteroanterior and lateral chest radiographs and chest CT (**A–C**) show left upper lobe consolidation with a similar appearance as bacterial community-acquired pneumonia. Enlarged left mediastinal lymph nodes are also present (**D**).

nodule, which can develop within a site of prior consolidation or from filling in of a prior cavity. Most nodules are 1 to 2 cm, but nodules of several centimeters can occur and can mimic lung cancer. The nodules are typically round, well-circumscribed, of homogeneous attenuation with variable borders (spiculated, lobulated, and smooth borders have all been observed), located in the lung periphery. Thin-walled cavitary lesions also can be seen, which can fluctuate in size secondary to ball-check mechanism trapping air within the cavity (Fig. 21) [59]. Patients with cavities may develop mycetomas, typically from aspergillus rather than from coccidioidomycosis itself. Although many patients with cavities are asymptomatic, patients may develop symptoms such as low-

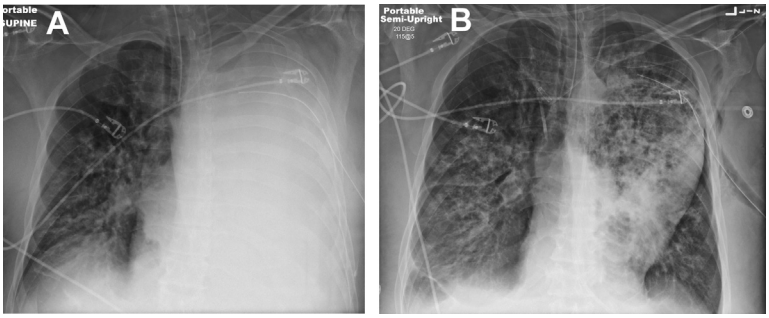


FIG. 19 Sixty-year-old man with coccidioidomycosis and empyema. Initial frontal chest radiograph (**A**) demonstrates a large left pleural effusion. A chest tube was placed (**B**), and residual bilateral consolidation and nodular opacities are present.

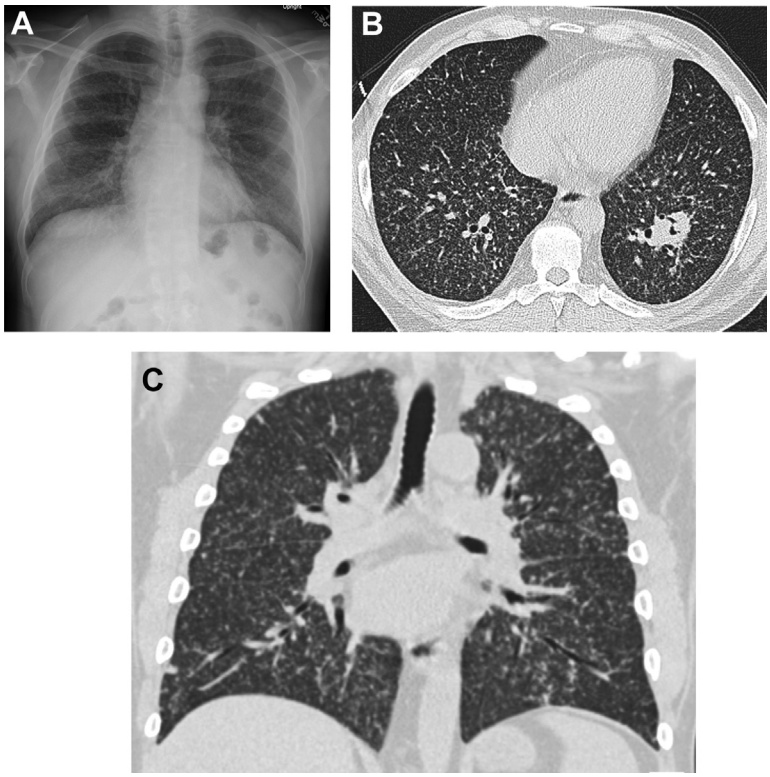


FIG. 20 Disseminated coccidioidomycosis in a 46-year-old man with prior renal transplant. Frontal chest radiograph (**A**), axial chest CT (**B**), and coronal chest CT (**C**) show innumerable bilateral randomly distributed miliary nodules. Focal left upper lobe consolidation is also demonstrated on CT (**B**).

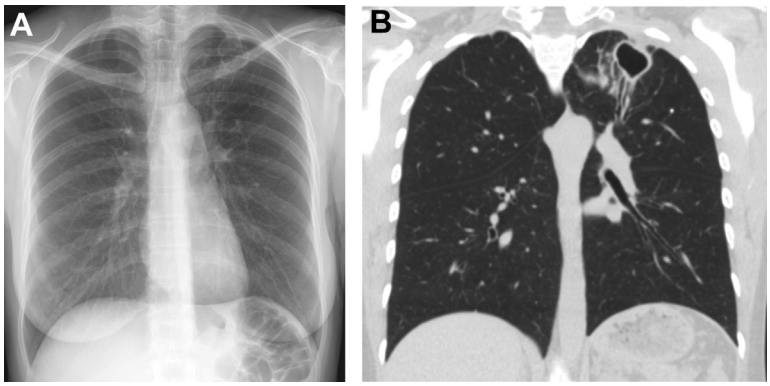


FIG. 21 Thin-walled cavity of chronic coccidioidomycosis in a 42-year-old-woman. Posteroanterior chest radiograph (**A**) and coronal CT (**B**) demonstrate left upper lobe thin-walled cavity with adjacent bronchiectasis and pleural thickening.

grade fever, weight loss, and hemoptysis if a mycetoma develops within the cavity or if there is bacterial superinfection of the cavity.

Fewer than 1% of patients can develop more complex-appearing chronic, fibrocavitary consolidation that mimics the appearance of tuberculosis, nontuberculosis mycobacterial disease, and histoplasmosis (Fig. 22). This fibrocavitary change is disproportionately seen in African American, Filipino, Latino, and American Indian individuals, and patients with diabetes [57]. Treatment is necessary and involves prolonged administration of oral azole antifungals [60].

Diagnosis of coccidiodomycosis depends on the acuity of the illness. Acute disease can be diagnosed with serum antigen testing for immunoglobulin (Ig)G and IgM antibodies and/or sputum culture. Relevant to chronic infections, residual nodules ("coccidioidomas") often contain viable organisms that can yield positive cultures. This is in contrast to some other endemic fungal infections, such as histoplasmosis, in which residual nodules are usually sterile [60]. Patients with chronic cavitary infection will typically have negative serum IgG and IgM antibodies, but will have positive sputum culture.

## NONTUBERCULOUS MYCOBACTERIA

NTMB, aside from "hot tub" lung, are associated with chronic rather than acute or subacute disease. Although indolent rather than epidemic, these pathogens are resilient and their prevalence and impact on world health has grown steadily in the twenty-first century. Disease prevalence in the United States has doubled in the past 2 decades and tripled in South Korea, most recently estimated at approximately 40 cases per 100,000 in the latter [61]. Increases in prevalence have been largely driven by increases in *Mycobacterium avium* complex (MAC) in North America and by *Mycobacterium abscessus* (MABS) in Asia. The latter organism, a member of the NTMBs classified as rapid growers, is less common than MAC worldwide, but causes significant morbidity due to their characteristic antibiotic resistance and poor response to treatment [62].

The reasons for the increasing prevalence are multifactorial. The NTMB cell wall is lipid rich and readily forms biofilms. It can resist disinfectants and is particularly adept at colonizing shower heads, where it readily forms aerosols. Recently, human-to-human transmission of a multidrug-resistant MABS strain has been documented [63]. Host susceptibility likely plays a major role in NTM growing prevalence as well. It has long been recognized that patients with preexisting cystic fibrosis (CF) and non-CF bronchiectasis are at risk for NTM infection, and even patients with CF transmembrane conductance regulator gene heterozygosity may be at increased risk [64]. Other structural lung disease, such as alpha-1-antitrypsin and lung cancer, may also increase infection risk. In addition, immunologic deficits play a major role in NTM susceptibility, including those deficits caused by the expanding use of tumor necrosis factor (TNF) inhibitors and other biologics in the treatment of autoimmune diseases [65]. Naturally occurring genetic variation, such as in alleles coding for TNF-alpha and specific interleukins likely affect an individual's susceptibility to NMT as well [66].

For the past 2 decades, MAC pulmonary infections may be classified into an (upper lobe) fibrocavitary lung disease seen mostly in male patients with underlying COPD, and a bronchiectatic form most commonly seen in women with slender body habitus and chest wall deformities [67] (Fig. 23). Recently a sophisticated latent class analysis suggested that NTMB morphologically might be divided into 3 groups that better define morbidity and mortality. The NTM group with the lowest morality manifested mild radiologic

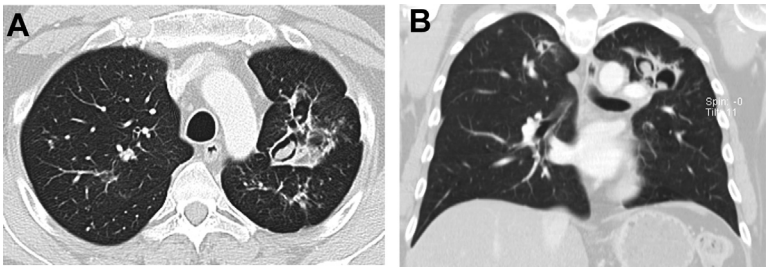


FIG. 22 Thin-walled cavity of chronic coccidioidomycosis with mycetoma in a 31-year-old man. Axial (**A**) and coronal (**B**) chest CT show left upper lobe thin-walled cavity with internal circumscribed nodules with smooth borders compatible with mycetoma.

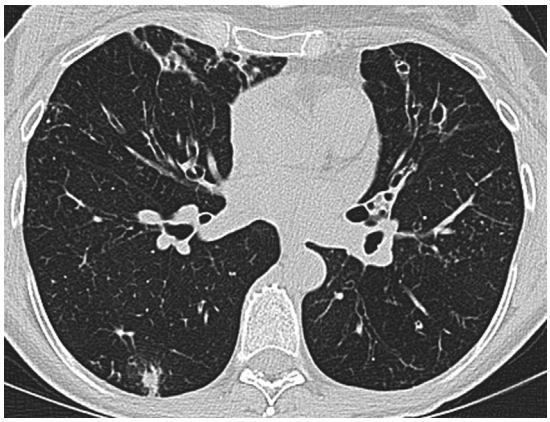

FIG. 23 Typical appearance of MAC. Axial chest CT in a 64-year-old woman demonstrates multifocal areas of cylindrical bronchiectasis, especially in the right middle lobe and lingula, with tree-in-bud centrilobular nodules and at least one larger discrete nodule.

abnormalities primarily confined to nodules, which were occasionally cavitary. A second group with intermediate mortality was defined as having extensive bronchiectasis and widespread tree-in-bud opacities. The third group demonstrated extensive cavities accompanied by moderate to severe bronchiectasis and had the highest mortality. This report is concordant with other studies showing that cavitary disease is associated with a much a higher 5-year mortality than patients whose manifestations of infection are confined to bronchiectasis and nodules (Fig. 24). Accordingly, the presence of cavitary disease generally warrants the initiation of treatment and necessitates a more intensive therapeutic regimen than used if treatment is initiated in noncavitary disease [67–70].

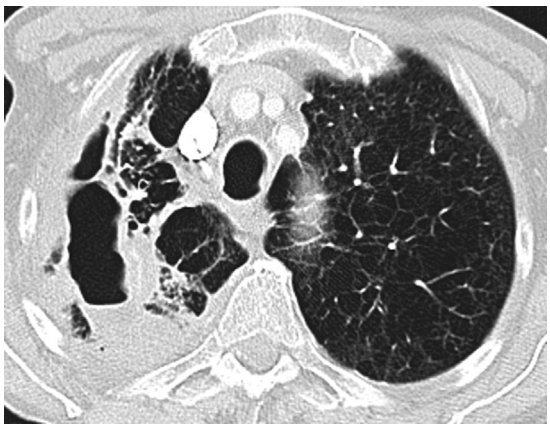

FIG. 24 Severe cavitary MAC in a 58-year-old man with emphysema. Axial chest CT shows a large, thick-walled right upper lobe cavity with adjacent consolidation and internal air-fluid level.

The radiologic manifestations of cavitary MAC are similar to tuberculosis, but do have subtle distinctions. Not surprisingly, when compared with patients with cavitary tuberculosis, patients with NTM cavitary lung disease are more likely to have widespread bronchiectasis. Compared with tuberculous cavities, MAC-infected cavities have thinner walls with less surrounding parenchymal opacities and tend to develop pleural thickening adjacent to the cavity (Fig. 25). In one study, pleural thickening adjacent to the cavity, right upper lobe bronchiectasis, and ill-defined tree-in-bud nodules all carried odds ratios greater than 5 for predicting NTMB over tuberculous infection [71].

As noted previously, bronchiectasis, with or without accompanying cavities, is the signature finding of NMT. Bronchiectasis may be caused by these pathogens or conversely, preexisting bronchiectasis may predispose to colonization and establishment of infection with NTMB. Bronchiectasis caused by MAC is typically most severe in the lingula and middle lobe, but is frequently present in other lobes as well, particularly the right upper lobe [72]. Interestingly, the ability to culture NMTB from the sputum is more closely related to the concurrent present of cavities rather than the extent of bronchiectasis [73].

Patients with mild underlying immune suppression, such as diabetes, and bronchiectatic NTM are more likely to demonstrate cavitary nodules and opacities >2 cm, than are immunocompetent hosts. Although there is considerable overlap in appearance of different NMTs, the distribution of bronchiectasis in *Myocbacterium abscessus* infection may not show the predilection for the middle lobe and lingula seen with MAC [74]. Another series suggested that *M abscessus* is more likely than MAC to manifest as the bronchiectatic nodular form rather than cavitary disease. When cavities were present in *M abscessus* infections, they were less likely to be thin walled [75] (Fig. 26).

## CHRONIC PULMONARY ASPERGILLOSIS

Chronic infection with aspergillus, like NMTB infection is being recognized with increasing frequency this century (Table 2). Chronic pulmonary aspergillosis (CPA) most often occurs in lung damaged from tuberculosis, occurring in 20% or more of patients with prior cavitary tuberculous disease. In areas of the world where the prevalence of tuberculosis is low, COPD has been the

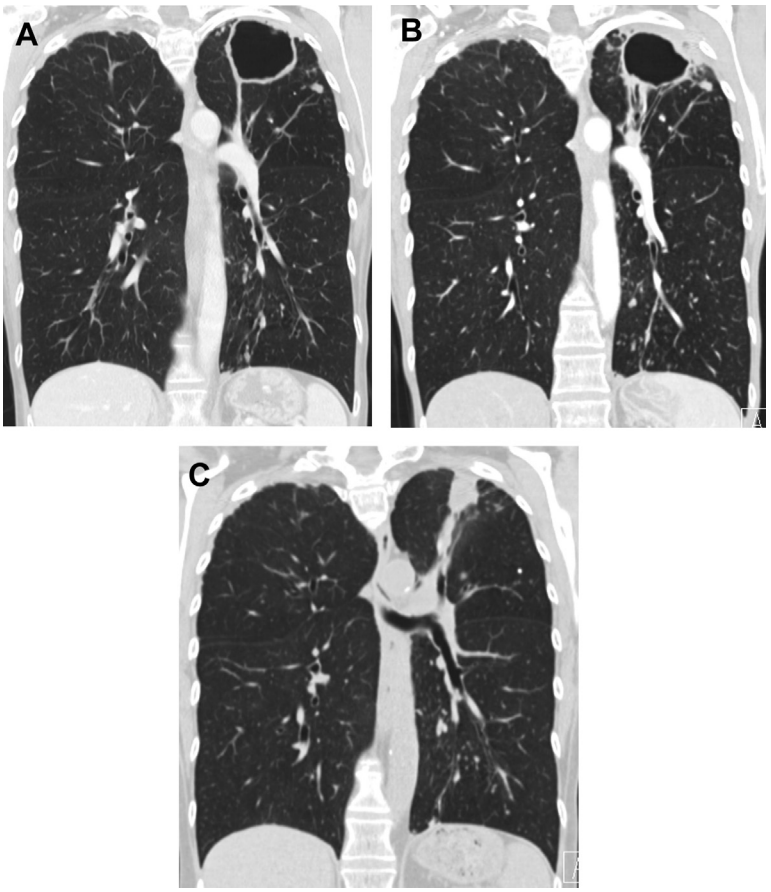


FIG. 25 Thin-walled cavitary MAC in a 56-year-old woman. Coronal chest CTs before treatment (**A, B**) show a thin-walled cavity that develops adjacent pleural thickening and nodularity. Coronal chest CT following treatment (**C**) shows collapse of the cavity with residual nodule.

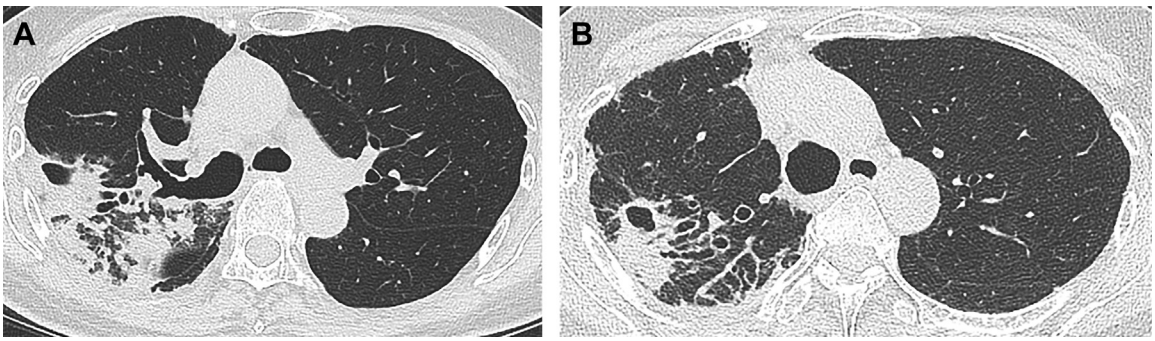


FIG. 26 *Mycobacterium abscessus* in a 50-year-old man. Axial chest CT (**A**) demonstrates largely thick-walled cavity and nearby bronchiectasis. Follow-up chest CT 4 years later (**B**) shows improvement in cavity size, but with increased bronchiectasis. (*From* Dr. Jane P. Ko, MD, New York University Langone Health; *with permission*.)

**TABLE 2**
**Chronic Emerging Thoracic Infections**

| Organism | Typical Imaging Finding | Additional Imaging Findings | Epidemiology |
|---|---|---|---|
| *Coccidioides* (chronic) | Nodules, thin-walled solitary cavities | Upper lobe fibrocavitary disease, rare | Endemic, fibrocavitary disease more common in specific ethnic groups |
| NTMB | Bronchiectasis, nodules (macronodules and tree in bud), cavities | Pleural thickening adjacent to cavities | Endemic, prevalence surpasses TB in the United States and Europe |
| *Aspergillus* | Expanding preexisting cavities or bullae with progressive adjacent parenchymal disease | Aspergillomas, adjacent pleural thickening | Seen in patients with COPD or NTMB in the United States and Europe, superimposed on TB elsewhere |

*Abbreviations:* COPD, chronic obstructive pulmonary disease; NTMB, nontuberculous mycobacteria; TB, tuberculosis.

predominant CPA risk factor due to associated bullous emphysema as well as the use of inhaled and/or systemic corticosteroids. More recently CPA infection has been recognized as an important sequela of NTMB infections, the 2 chronic infections co-emerging in many parts of the world [76]. In the United Kingdom, for example, approximately equal percentages of CPA cases occur in the setting of prior NTMB infection as in the setting of prior tuberculosis (TB). Although characteristically associated with the NTMB classic pattern, CPA can also occur in conjunction with bronchiectatic pattern of NTMB infection [77].

CPA is an infection characterized by a tissue invasion less severe than seen in angioinvasive aspergillosis but more extensive than seen with aspergillomas or allergic bronchopulmonary aspergillosis. Infectious disease literature often divides this umbrella term into (1) subacute invasive aspergillosis (when the disease develops rapidly, in <3 months); (2) chronic cavitary pulmonary aspergillosis (when then disease develops more slowly); and (3) fibrosing aspergillosis (when extensive fibrosis, often asymmetric, is present) [77,78]. Because these distinctions can be difficult to make radiologically, radiologists may prefer the more general term of CPA [79].

Radiologic presentation of CPA is influenced by the underlying disease. When superimposed on preexisting COPD, the disease can present as persistent consolidation in the upper lobes that develops cavitation and results in single or multiple thick-walled or thin-walled upper lobe cavities that slowly increase in size [80] (Fig. 27). Progression of upper lobe cavitary disease is associated with local architectural distortion but

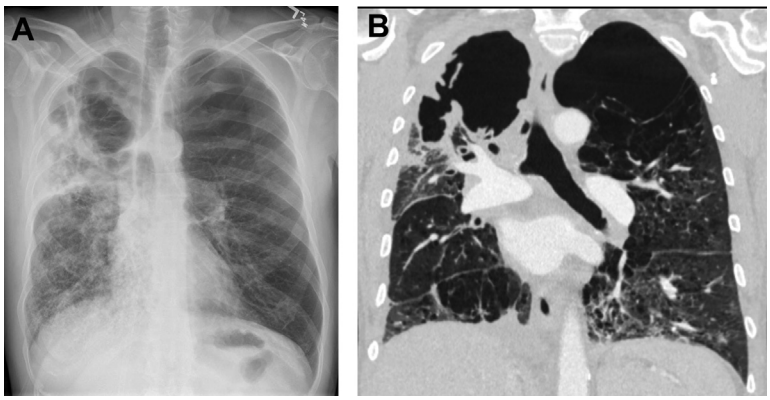


FIG. 27 Chronic cavitary aspergillosis in a 62-year-old man with emphysema. Chest radiograph (**A**) and coronal chest CT (**B**) show an irregular relatively thick-walled cavity with adjacent pleural thickening. Nodules can also be seen in the right lower lung (**A**) and left lower lung (**B**).

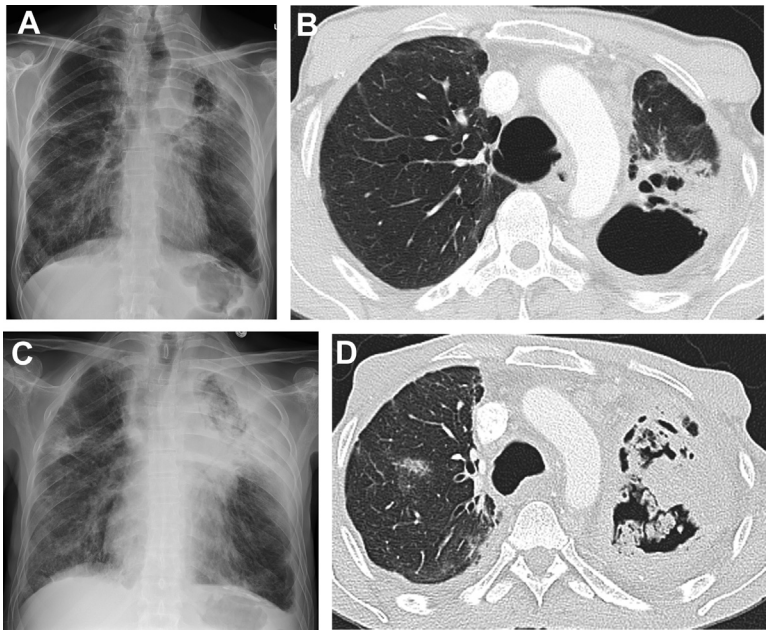


FIG. 28 Progression of chronic aspergillosis in a 49-year-old man with underlying emphysema. Chest radiograph (**A**) and axial chest CT (**B**) show thick-walled left upper lobe cavity with adjacent consolidation. Several months later, chest radiograph (**C**) and chest CT (**D**) show marked increase in cavity wall thickness, internal aspergilloma formation, and adjacent pleural thickening.

extensive fibrosis can also occur into the adjacent lobes, often asymmetrically (Fig. 28). In the setting of CPA, irregular wall thickening with a cavity ("scablike" sign) has been associated with hemoptysis [81].

When CPA is superimposed on previous classic NTMB or tuberculosis, it results in extension of preexisting cavities and adjacent fibrosis that mimics progression of the underlying disease. In the case of NTMB, development of chronic aspergillosis usually occurs more than a year after NMTB infection is diagnosed. Radiologic signs of aspergillosis superimposed on mycobacterial infection include pleural thickening adjacent to the areas of consolidation or cavitation and aspergilloma formation [76]. Pleural thickening usually presages the appearance of the aspergilloma, which may be multiple (Figs. 29 and 30).

Imaging findings suggesting chronic aspergillosis should drive laboratory evaluation focused on that diagnosis. Despite the presence of cavitary disease, culture of respiratory secretions for aspergillus may be positive in only 50% of patients. Cultures of *Aspergillus fumigatus* are more likely to be true positives compared with nonfumigatus species. The latter are less likely to be true pathogens, possibly because the larger size of these species impedes penetration into alveoli. Fortunately, serum-specific IgG is positive in 90% of all chronic aspergillus

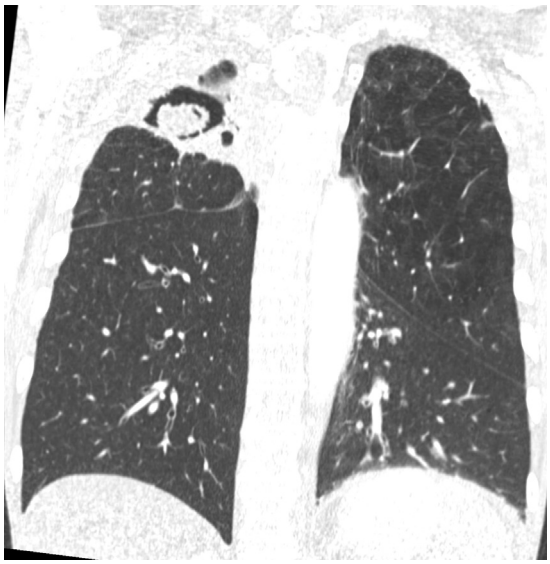

FIG. 29 Chronic aspergillosis superimposed on nontuberculous mycobacterial infection in a 57-year-old man. Extensive pleural thickening is present adjacent to the right upper lobe cavity, and an aspergilloma is also conspicuous. (*From* Dr. Jeffrey P. Kanne, MD, University of Wisconsin School of Medicine and Public Health; *with permission*.)

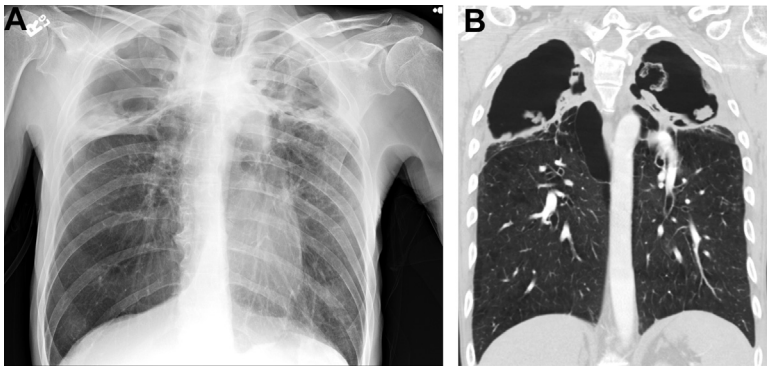


FIG. 30 Aspergilloma in a 65-year-old man. Frontal chest radiograph (**A**) and coronal chest CT (**B**) show bilateral thick-walled apical cavities with internal debris including an organized aspergilloma on the left. (*From* [*A*] Ketai L, Currie BJ, Holt MR, Chan ED. Radiology of Chronic Cavitary Infections. J Thorac Imaging. 2018 Sep;33(5):334–343. PMID: 30048346; *with permission*.)

infections [60]. Treatment usually involves long-term triazole therapy but can be complicated by drug-drug interactions if patients are receiving rifamycin group antibiotics. This drug interaction occurs more commonly in patients with NMTB than in those with TB due to the longer duration of treatment and may contribute to the higher mortality of CPA in the setting of NMTB.

## SUMMARY

Emerging infections can cause acute or chronic disease and be epidemic or insidious in their spread. Their emergence can be driven by changes in the organism or changes in the human population and its environment. Both are changing constantly. This paper has attempted to address imaging questions relevant to several emerging infections commonly seen in current clinical practice in North American, Europe, and northeast Asia. Other major pathogens, many of them parasitic (eg, Chagas disease, stronglydiasis) are reemerging in other regions of the world and have a profound effect on global health. These and yet unknown emerging pathogens will continue to challenge diagnostic imaging in the remainder of the twenty-first century.

## DISCLOSURE

The authors have no commercial or financial conflicts of interest.

## REFERENCES

[1] Tai W, He L, Zhang X, et al. Characterization of the receptor-binding domain (RBD) of 2019 novel coronavirus: implication for development of RBD protein as a viral attachment inhibitor and vaccine. Cell Mol Immunol 2020;17(6):613–20.

[2] Bouri N, Sell TK, Franco C, et al. Return of epidemic dengue in the United States: implications for the public health practitioner. Public Health Rep 2012;127(3):259–66.

[3] Prokop M, van Everdingen W, van Rees Vellinga T, et al, COVID-19 Standardized Reporting Working Group of the Dutch Radiological Society. CO-RADS: a categorical CT assessment scheme for patients suspected of having COVID-19-definition and evaluation. Radiology 2020;296(2):E97–104.

[4] Simpson S, Kay FU, Abbara S, et al. Radiological Society of North America Expert Consensus Statement on Reporting Chest CT Findings Related to COVID-19. Endorsed by the Society of Thoracic Radiology, the American College of Radiology, and RSNA - Secondary Publication. J Thorac Imaging 2020;35(4):219–27.

[5] Litmanovich DE, Chung M, R Kirkbride R, et al. Review of chest radiograph findings of COVID-19 pneumonia and suggested reporting language. J Thorac Imaging 2020;35(6):354–60.

[6] Kory P, Kanne JP. SARS-CoV-2 organizing pneumonia: 'Has there been a widespread failure to identify and treat this prevalent condition in COVID-19?'. BMJ Open Respir Res 2020;7(1):e000724.

[7] Kwee RM, Adams HJA, Kwee TC. Diagnostic performance of CO-RADS and the RSNA classification system in evaluating COVID-19 at chest CT: a meta-analysis. Radiol Cardiothorac Imaging 2021;3(1):e200510.

[8] Bai HX, Hsieh B, Xiong Z, et al. Performance of radiologists in differentiating COVID-19 from non-COVID-19 viral pneumonia at chest CT. Radiology 2020;296(2):E46–54.

[9] Wikramaratna PS, Paton RS, Ghafari M, et al. Estimating the false-negative test probability of SARS-CoV-2 by RT-PCR. Euro Surveill 2020;25(50):2000568.

[10] Libster R, Pérez Marc G, Wappner D, et al, INFANT–COVID-19 Group. Early high-titer plasma therapy to prevent severe COVID-19 in older adults. N Engl J Med 2021;384(7):610–8.
[11] Cavagna E, Muratore F, Ferrari F. Pulmonary thromboembolism in COVID-19: venous thromboembolism or arterial thrombosis? Radiol Cardiothorac Imaging 2020;2(4):e200289.
[12] van Dam LF, Kroft LJM, van der Wal LI, et al. Clinical and computed tomography characteristics of COVID-19 associated acute pulmonary embolism: a different phenotype of thrombotic disease? Thromb Res 2020;193:86–9.
[13] Oudkerk M, Kuijpers D, Oudkerk SF, et al. The vascular nature of COVID-19. Br J Radiol 2020;93(1113): 20200718.
[14] Lang M, Som A, Carey D, et al. Pulmonary vascular manifestations of COVID-19 pneumonia. Radiol Cardiothorac Imaging 2020;2(3):e200277.
[15] Rawson TM, Moore LSP, Zhu N, et al. Bacterial and fungal coinfection in individuals with coronavirus: a rapid review to support COVID-19 antimicrobial prescribing. Clin Infect Dis 2020;71(9):2459–68.
[16] McGuinness G, Zhan C, Rosenberg N, et al. Increased incidence of barotrauma in patients with COVID-19 on invasive mechanical ventilation. Radiology 2020; 297(2):E252–62.
[17] Rogliani P, Calzetta L, Coppola A, et al. Are there pulmonary sequelae in patients recovering from COVID-19? Respir Res 2020;21:286.
[18] Guler SA, Ebner L, Beigelman C, et al. Pulmonary function and radiological features four months after COVID-19: first results from the national prospective observational Swiss COVID-19 lung study. Eur Respir J 2021;57(4):2003690.
[19] Han X, Fan Y, Alwalid O, et al. Six-month follow-up chest CT findings after severe COVID-19 pneumonia. Radiology 2021;299(1):E177–86.
[20] Carfì A, Bernabei R, Landi F, Gemelli Against COVID-19 Post-Acute Care Study Group. Persistent symptoms in patients after acute COVID-19. JAMA 2020;324(6):603–5.
[21] Cheng VC, To KK, Tse H, et al. Two years after pandemic influenza A/2009/H1N1: what have we learned? Clin Microbiol Rev 2012;25(2):223–63.
[22] Centers for Disease Control and Prevention. The burden of the influenza A H1N1pdm09 virus since the 2009 pandemic. 2019. Available at: https://www.cdc.gov/flu/pandemic-resources/burden-of-h1n1.html. Accessed March 31, 2021.
[23] Agarwal PP, Cinti S, Kazerooni EA. Chest radiographic and CT findings in novel swine-origin influenza A (H1N1) virus (S-OIV) infection. AJR Am J Roentgenol 2009;193(6):1488–93.
[24] Koo HJ, Lim S, Choe J, et al. Radiographic and CT features of viral pneumonia. Radiographics 2018;38(3): 719–39.
[25] Miller WT Jr, Mickus TJ, Barbosa E Jr, et al. CT of viral lower respiratory tract infections in adults: comparison among viral organisms and between viral and bacterial infections. AJR Am J Roentgenol 2011;197(5):1088–95.
[26] Franquet T. Imaging of pulmonary viral pneumonia. Radiology 2011;260(1):18–39.
[27] Marchiori E, Zanetti G, D'Ippolito G, et al. Swine-origin influenza A (H1N1) viral infection: thoracic findings on CT. AJR Am J Roentgenol 2011;196(6):W723–8.
[28] Yin Z, Kang Z, Yang D, et al. A comparison of clinical and chest CT findings in patients with influenza A (H1N1) virus infection and coronavirus disease (COVID-19). AJR Am J Roentgenol 2020;215(5):1065–71.
[29] Shafagati N, Williams J. Human metapneumovirus - what we know now. F1000Res 2018;7:135.
[30] Kahn JS. Human metapneumovirus: a newly emerging respiratory pathogen. Curr Opin Infect Dis 2003;16(3):255–8.
[31] Panda S, Mohakud NK, Pena L, et al. Human metapneumovirus: review of an important respiratory pathogen. Int J Infect Dis 2014;25:45–52.
[32] Schildgen V, van den Hoogen B, Fouchier R, et al. Human metapneumovirus: lessons learned over the first decade. Clin Microbiol Rev 2011;24(4):734–54.
[33] Jain S, Self WH, Wunderink RG, et al, CDC EPIC Study Team. Community-acquired pneumonia requiring hospitalization among U.S. adults. N Engl J Med 2015; 373(5):415–27.
[34] Vidaur L, Totorika I, Montes M, et al. Human metapneumovirus as cause of severe community-acquired pneumonia in adults: insights from a ten-year molecular and epidemiological analysis. Ann Intensive Care 2019; 9(1):86.
[35] Marinari LA, Danny MA, Simpson SA, et al. Lower respiratory tract infection with human metapneumovirus: chest CT imaging features and comparison with other viruses. Eur J Radiol 2020;128:108988.
[36] Mercante JW, Winchell JM. Current and emerging legionella diagnostics for laboratory and outbreak investigations. Clin Microbiol Rev 2015;28(1):95–133.
[37] Centers for Disease Control and Prevention. What clinicians need to know about Legionnaire's disease. 2020. Available at: https://www.cdc.gov/legionella/downloads/fs-legionella-clinicians.pdf. Accessed March 15, 2020.
[38] Collier SA, Deng L, Adam EA, et al. Estimate of burden and direct healthcare cost of infectious waterborne disease in the United States. Emerg Infect Dis 2021;27(1): 140–9.
[39] Neil K, Berkelman R. Increasing incidence of legionellosis in the United States, 1990–2005: changing epidemiologic trends. Clin Infect Dis 2008;47(5):591–9.
[40] Centers for Disease Control and Prevention. Legionnaires' disease surveillance summary report, 2014–2015 [pdf]. 2018. Available at: https://www.cdc.gov/legionella/health-depts/surv-reporting/2014-15-surv-report-508.pdf. Accessed March 15, 2020.
[41] Sopena N, Pedro-Botet ML, Sabrià M, et al. Comparative study of community-acquired pneumonia caused by *Streptococcus pneumoniae*, *Legionella pneumophila* or *Chlamydia pneumoniae*. Scand J Infect Dis 2004;36(5):330–4.

[42] Nelson KN, Binney ZO, Chamberlain AT. Excess pneumonia mortality during a 2014-2015 legionnaires' disease outbreak in Genesee County, Michigan. Epidemiology 2020;31(6):823–31.
[43] Faccini M, Russo AG, Bonini M, et al. Large community-acquired Legionnaires' disease outbreak caused by *Legionella pneumophila* serogroup 1, Italy, July to August 2018. Euro Surveill 2020;25(20):1900523.
[44] Kessler MA, Osman F, Marx J Jr, et al. Hospital-acquired legionella pneumonia outbreak at an academic medical center: lessons learned. Am J Infect Control 2021. https://doi.org/10.1016/j.ajic.2021.02.013.
[45] Weiss D, Boyd C, Rakeman JL, et al. A large community outbreak of legionnaires' disease associated with a cooling tower in New York City, 2015. Public Health Rep 2017;132(2):241–50.
[46] Rabooki T, Hashemi SH, Rabooki D, et al. Evaluation of epidemiological and clinical features of patients with pneumococcal and legionella pneumonia. Biomed Biotechnol Res J 2019;3(3):176–81.
[47] Tan MJ, Tan JS, Hamor RH, et al. The radiologic manifestations of legionnaire's disease. The Ohio community-based pneumonia incidence study group. Chest 2000; 117(2):398–403.
[48] Poirier R, Rodrigue J, Villeneuve J, et al. Early radiographic and tomographic manifestations of legionnaires' disease. Can Assoc Radiol J 2017;68(3):328–33.
[49] Maillet F, Bonnet N, Billard-Pomares T, et al. Fatal legionella pneumophila serogroup 1 pleural empyema: a case report. World J Crit Care Med 2019;8(6):99–105.
[50] Nakanishi M, Shiroshita A, Nakashima K, et al. Clinical and computed tomographic features of Legionella pneumonia with negative urine antigen test results. Respir Investig 2021;59(2):204–11.
[51] Sakai F, Tokuda H, Goto H, et al. Computed tomographic features of *Legionella pneumophila* pneumonia in 38 cases. J Comput Assist Tomogr 2007;31(1):125–31.
[52] Haroon A, Higa F, Hibiya K, et al. Organizing pneumonia pattern in the follow-up CT of Legionella-infected patients. J Infect Chemother 2011;17(4):493–8.
[53] Di Stefano F, Verna N, Di Gioacchino M. Cavitary legionella pneumonia in a patient with immunodeficiency due to hyper-IgE syndrome. J Infect 2007; 54(3):e121–3.
[54] Hamm PS, Hutchison MI, Leonard P, et al. First analysis of human coccidioides isolates from New Mexico and the Southwest Four Corners region: implications for the distributions of *C. posadasii* and *C. immitis* and human groups at risk. J Fungi (Basel) 2019;5(3):74.
[55] Ampel NM. Coccidioidomycosis: changing concepts and knowledge gaps. J Fungi (Basel) 2020;6(4):354.
[56] McCotter O, Kennedy J, McCollum J, et al. Coccidioidomycosis among American Indians and Alaska natives, 2001–2014. Open Forum Infect Dis 2019;6(3).
[57] Jude CM, Nayak NB, Patel MK, et al. Pulmonary coccidioidomycosis: pictorial review of chest radiographic and CT findings. Radiographics 2014;34(4):912–25.
[58] Donovan FM, Zangeneh TT, Malo J, et al. Top questions in the diagnosis and treatment of coccidioidomycosis. Open Forum Infect Dis 2017;4(4):ofx197.
[59] Ketai L, Currie BJ, Holt MR, et al. Radiology of chronic cavitary infections. J Thorac Imaging 2018;33(5):334–43.
[60] Holt MR, Chan ED. Chronic cavitary infections other than tuberculosis: clinical aspects. J Thorac Imaging 2018;33(5):322–33.
[61] Lee H, Myung W, Koh WJ, et al. Epidemiology of nontuberculous mycobacterial infection, South Korea, 2007-2016. Emerg Infect Dis 2019;25(3):569–72.
[62] Lee M-R, Sheng W-H, Hung C-C, et al. Mycobacterium abscessus complex infections in humans. Emerging Infect Dis 2015;21(9):1638–46.
[63] Bryant JM, Grogono DM, Rodriguez-Rincon D, et al. Emergence and spread of a human-transmissible multidrug-resistant nontuberculous mycobacterium. Science 2016;354(6313):751–7.
[64] Szymanski EP, Leung JM, Fowler CJ, et al. Pulmonary nontuberculous mycobacterial infection. A multisystem, multigenic disease. Am J Respir Crit Care Med 2015; 192(5):618–28.
[65] Ratnatunga CN, Lutzky VP, Kupz A, et al. The rise of non-tuberculosis mycobacterial lung disease. Front Immunol 2020;11:303.
[66] Affandi JS, Hendry S, Waterer G, et al. Searching for an immunogenetic factor that will illuminate susceptibility to non-tuberculous mycobacterial disease. Hum Immunol 2013;74(10):1382–5.
[67] Aksamit TR1, Philley JV2, Griffith DE. Nontuberculous mycobacterial (NTM) lung disease: the top ten essentials. Respir Med 2014;108(3):417–25.
[68] Lam PK, Griffith DE, Aksamit TR, et al. Factors related to response to intermittent treatment of *Mycobacterium avium* complex lung disease. Am J Respir Crit Care Med 2006;173:1283–9.
[69] Wallace RJ Jr, Brown-Elliott BA, McNulty S, et al. Macrolide/Azalide therapy for nodular/bronchiectatic mycobacterium avium complex lung disease. Chest 2014; 146:276–82.
[70] Ito Y, Hirai T, Maekawa K, et al. Predictors of 5-year mortality in pulmonary *Mycobacterium avium*-intracellulare complex disease. Int J Tuberc Lung Dis 2012;16(3): 408–14.
[71] Kim C1 2, Park SH3, Oh SY1, et al. Comparison of chest CT findings in nontuberculous mycobacterial diseases vs. *Mycobacterium tuberculosis* lung disease in HIV-negative patients with cavities. PLoS One 2017;12(3):e0174240.
[72] Choi S, Richards JC, Chan ED. Can physics principles help explain why non-tuberculous mycobacterial lung disease is more severe in the right middle lobe and lingula? J Thorac Dis 2019;11(11):4847–54.
[73] Lynch DA, Simone PM, Fox MA, et al. CT features of pulmonary *Mycobacterium avium* complex infection. J Comput Assist Tomogr 1995;19(3):353–60.
[74] Han D, Lee KS, Koh WJ, et al. Radiographic and CT findings of nontuberculous mycobacterial pulmonary

infection caused by mycobacterium abscessus. AJR Am J Roentgenol 2003;181(2):513–7.

[75] Chung MJ, Lee KS, Koh WJ, et al. Thin section CT findings of nontuberculous mycobacterial pulmonary diseases: comparison between *Mycobacterium avium*-intracellulare complex and *Mycobacterium abscessus* infection. J Korean Med Sci 2005;20(5):777–83.

[76] Phoompoung P, Chayakulkeeree M. Chronic pulmonary aspergillosis following nontuberculous mycobacterial infections: an emerging disease. J Fungi (Basel) 2020;6(4):346.

[77] Denning DW, Cadranel J, Beigelman-Aubry C, et al. Chronic pulmonary aspergillosis: rationale and clinical guidelines for diagnosis and management. Eur Respir J 2016;47(1):45–68.

[78] Kosmidis C, Denning DW. The clinical spectrum of pulmonary aspergillosis. Thorax 2015;70:270–7.

[79] Desai SR, Hedayati PK, Hansell DM. Chronic aspergillosis of the lungs: unravelling the terminology and radiology. Eur Radiol 2015;25:3100–7.

[80] Hayes GE, Novak-Frazer L. Chronic pulmonary aspergillosis—where are we? and where are we going? J Fungi 2016;2(18):1–34.

[81] Sato H, Okada F, Matsumoto S, et al. The scab-like sign: a CT finding indicative of haemoptysis in patients with chronic pulmonary aspergillosis? Eur Radiol 2018;28(10):4053–61.